

# Supporting Information

Lee et al. 10.1073/pnas.1004602107

## SI Materials and Methods

**Statistical Analysis of ChIP-Chip Data.** ChIP-chip data were analyzed using the moving average (MA) method in TileMapv2 (1). Gli1-bound regions (or peaks) were ranked according to the MA statistic. Briefly, for each probe, a variance stabilized *t* statistic was computed to measure the difference between chromatin immunoprecipitation (chIP) and control probe intensities. Then an MA statistic was computed for each probe by averaging all *t* statistics within a 300 bp flanking window of the probe. Probes with an MA statistic  $\geq 2.5$  were used to predict Gli1-bound regions. To determine the between-experiment variation in the number of peaks, we performed a bootstrap analysis to analyze three chIP and three control samples. Forty-nine new experiments with three chIP and three control samples were simulated by sampling the available chIP and control samples with replacement. Each simulated experiment was analyzed by using the same peak detection procedure. According to this analysis, there are  $3,514 \pm 220$  (mean  $\pm$  SE) granule neuron precursor cell (GNP) regions and  $4,486 \pm 116$  medulloblastoma (MB) regions.

The false-discovery rate (FDR) was determined using three different approaches. First, FDR for each peak list was determined using the MA statistics. Second, CisGenome was used to map Gli motifs to each region. To effectively control for biases that may affect motif analysis (2), “matched control regions” were randomly selected such that the distance between the control region and the closest transcription start site (TSS) has the same probability distribution as the distance between the TileMap ranked peak and the TSS. TileMap ranked peaks were then grouped into bins of 1,000 peaks. For each bin, we computed the motif enrichment as the ratio between the Gli motif occurrence rate (i.e., number of motif sites per 1 kb) in TileMap ranked peaks and the Gli motif occurrence rate in control regions. The ratio for each bin is plotted in Fig. S2 A and B.

In the third analysis, FDR was determined by performing quantitative PCR (qPCR) on selected regions (as described in the main text). At least nine regions per bin of 1,000 ranked regions were chosen randomly and assayed by qPCR (Fig. S2 C and D). For each region tested by qPCR, a local FDR was derived from the number of false-positive results among 10 assayed regions with the closest rankings. Local FDR cutoff was 50%. High-confidence Gli1-bound regions

passed all three FDR analyses. Primers used for ChIP-qPCR are listed in Table S7. ChIP-chip data are accessible through GEO Series accession no. GSE17682 in the National Center for Biotechnology Information's Gene Expression Omnibus (3).

CisGenome (4) was used to annotate each Gli1 binding regions to the closest TSS, compute genomic distributional properties, extract conservation scores, perform de novo motif discovery, and map motif sites to genomes. Conservation of the 500 bp around Gli1 peak maxima was assessed using the average phastCons score across 17 vertebrate species (University of California Santa Cruz genome browser) (5).

**Gli1 Binding and Expression Data Analysis.** Entrez gene IDs were used to identify and compare genes from Exon array and ChIP-chip analyses. Statistical significance of the intersection was calculated by the hypergeometric distribution, and fold enrichment was calculated by the ratio of observed vs. expected genes in the intersection. Four parameters were used for an integrated analysis of the Gli1 target genes: genes expressed in GNPs, genes expressed in MBs, genes with nearby Gli1 binding in GNPs, and genes associated with Gli1 binding in MBs. Every combination was examined (Fig. 2 in main text).

**In Situ Hybridization.** Tissues for in situ hybridization were fixed in 4% paraformaldehyde, sunk in 30% sucrose/PBS, and embedded in OCT (Tissue-Tek). Midline sagittal sections (10–20  $\mu$ m) were hybridized with digoxigenin-labeled riboprobes at 62–68°C. Anti-digoxigenin antibody (Roche) and 4-Nitro blue tetrazolium chloride (NBT) and 5-Bromo-4-chloro-3-indolyl-phosphate (BCIP) (Roche) were used for detection. The probes for *Gli1*, *Olig1*, and *Olig2* are previously described (6, 7). Other probes used are as follows: *Akna* (nucleotides 3578–4108 of NM\_001045514.2), *Cltb* (nucleotides 80–1468 of NM\_028870), *Gpr153* (nucleotides 1944–2639 of BC037650), and *Nptx1* (nucleotides 2750–3494 of NM\_008730.2). For immunostaining immediately after *Cltb* in situ hybridization, sections were washed extensively in water, blocked with 10% goat serum (Vector Laboratories) in PBS and 0.1% Triton X-100, and incubated with anti-Calbindin antibody (Sigma).

1. Ji H, Wong WH (2005) TileMap: Create chromosomal map of tiling array hybridizations. *Bioinformatics* 21:3629–3636.
2. Ji H, Vokes SA, Wong WH (2006) A comparative analysis of genome-wide chromatin immunoprecipitation data for mammalian transcription factors. *Nucleic Acids Res* 34:e146.
3. Edgar R, Domrachev M, Lash AE (2002) Gene Expression Omnibus: NCB gene expression and hybridization array data repository. *Nucleic Acids Res* 30:207–210.
4. Ji H, et al. (2008) An integrated software system for analyzing ChIP-chip and ChIP-seq data. *Nat Biotechnol* 26:1293–1300.

5. Siepel A, et al. (2005) Evolutionarily conserved elements in vertebrate, insect, worm, and yeast genomes. *Genome Res* 15:1034–1050.
6. Wechsler-Reya RJ, Scott MP (1999) Control of neuronal precursor proliferation in the cerebellum by Sonic Hedgehog. *Neuron* 22:103–114.
7. Ye F, et al. (2009) HDAC1 and HDAC2 regulate oligodendrocyte differentiation by disrupting the beta-catenin-TCF interaction. *Nat Neurosci* 12:829–838.

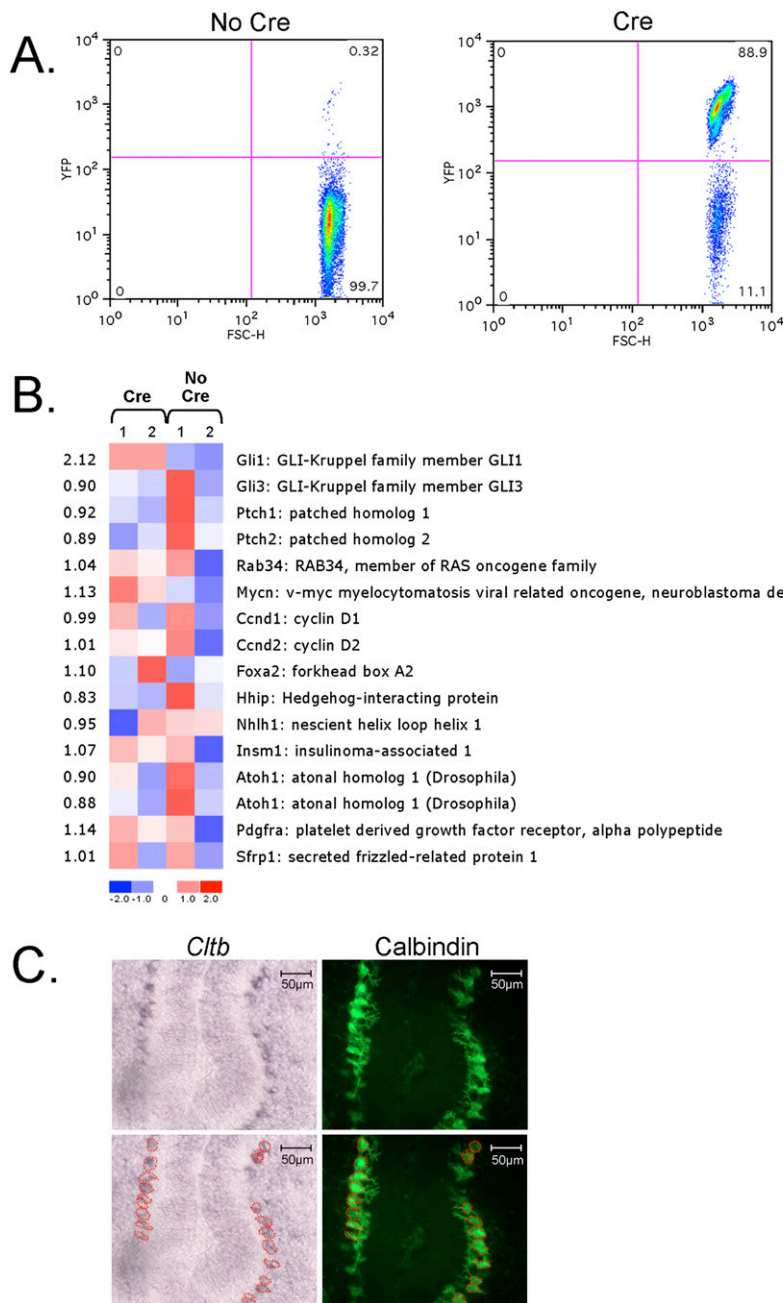


**Fig. S1.** (A and B) Analysis of GNPs expressing Gli1-FLAG. (A) Postnatal day 8 (P8) GNPs were isolated by percoll fractionation and analyzed by flow cytometry. In control GNPs (No Cre), 0.3% of cells were YFP positive (Left). In contrast, 89% of GNPs purified from *Rosa<sup>Gli1-FLAG/Gli1-FLAG</sup>;Math1-Cre/+* animals (Cre) were YFP positive (Right). The majority of *Rosa<sup>Gli1-FLAG/Gli1-FLAG</sup>;Math1-Cre/+* GNPs express YFP, and therefore Gli1-FLAG. GNPs used throughout this study were prepared in this manner. (B) Gene expression data for select genes from GNPs isolated from *Rosa<sup>Gli1-FLAG/Gli1-FLAG</sup>* mice (No Cre) and *Rosa<sup>Gli1-FLAG/Gli1-FLAG</sup>;Math1-Cre/+* (Cre). Fold change values (Cre vs. No Cre) are indicated on the left. Only *Gli1* levels are significantly increased (fold change >2) in the Cre GNPs. (C) *Cltb* is expressed in Purkinje cells in the developing cerebellum. In situ hybridization for *Cltb* in P6 cerebellar sagittal section (Left) shows that *Cltb* is not expressed in GNPs but is present in an internal layer of the cerebellum. The section was costained with an antibody against Calbindin, a Purkinje cell marker (Right), and the positively stained Purkinje cells are outlined (Lower Right). The outline was superimposed on the in situ pattern to reveal coincident localization of *Cltb* transcript and Purkinje cells (Lower Left).

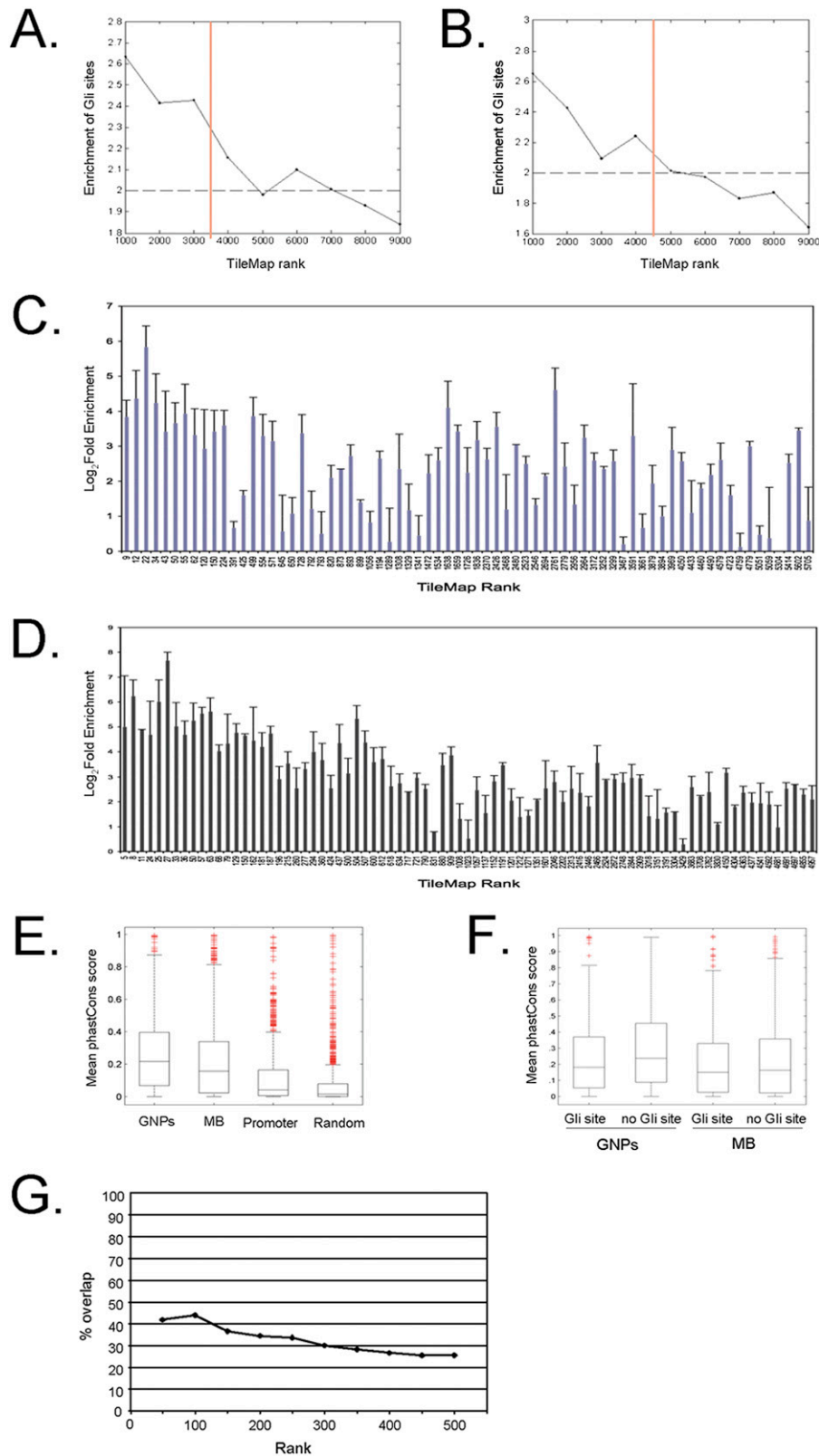


**Fig. S2.** Characterization of Gli1-bound regions. Gli motif enrichment analysis among all Gli1-bound regions in (A) GNPs and (B) MBs. For both cell types, an enrichment level of two was a secondary cutoff imposed on all TileMap ranked Gli1-bound regions (dotted line). At 5% FDR cutoff (orange vertical line), 3,514 and 4,486 regions were obtained. Validation of Gli1-bound regions by qPCR on unamplified ChIP samples in (C) GNPs and (D) tumors. Mean fold enrichment ( $\pm$  SE) of the indicated regions after Gli1-FLAG ChIP, as compared with total chromatin input, was determined for two to four biological replicates. (E) Box plots illustrate the level of evolutionary conservation (as assessed by mean phastCons scores) for the high-confidence Gli1-bound regions in GNPs and MBs. The Gli1-bound regions are highly conserved relative to promoter and random control sequences. (F) Conservation levels of Gli1-bound regions containing a Gli binding

Legend continued on following page

motif are similar to those lacking a Gli motif in both cell types. (G) The percentage of Gli1-bound regions shared between GNPs and MBs is shown as a function of the TileMap rankings. The moderate degree of overlap is similar across all ranked Gli1-bound regions in the two cell types.

## Other Supporting Information Files

[Table S1 \(XLS\)](#)

[Table S2 \(DOC\)](#)

[Table S3 \(DOC\)](#)

[Table S4 \(DOC\)](#)

[Table S5 \(XLS\)](#)

[Table S6 \(XLS\)](#)

[Table S7 \(XLS\)](#)